



Article

Fixed-Time Synchronization for Fractional-Order Cellular Inertial Fuzzy Neural Networks with Mixed Time-Varying Delays

Yeguo Sun ¹, Yihong Liu ^{2,*} and Lei Liu ²¹ School of Finance and Mathematics, Huainan Normal University, Huainan 232038, China; yeguosun@126.com² School of Computer Science, Huainan Normal University, Huainan 232038, China; leiliu2022@126.com

* Correspondence: liuyh@hnnu.edu.cn

Abstract: Due to the widespread application of neural networks (NNs), and considering the respective advantages of fractional calculus (FC), inertial neural networks (INNs), cellular neural networks (CNNs), and fuzzy neural networks (FNNs), this paper investigates the fixed-time synchronization (FDTS) issues for a particular category of fractional-order cellular-inertial fuzzy neural networks (FCIFNNs) that involve mixed time-varying delays (MTDs), including both discrete and distributed delays. Firstly, we establish an appropriate transformation variable to reformulate FCIFNNs with MTD into a differential first-order system. Then, utilizing the finite-time stability (FETS) theory and Lyapunov functionals (LFs), we establish some new effective criteria for achieving FDTS of the response system (RS) and drive system (DS). Eventually, we offer two numerical examples to display the effectiveness of our proposed synchronization strategies. Moreover, we also demonstrate the benefits of our approach through an application in image encryption.

Keywords: FDTS; FCIFNNs; LF; MTD

Citation: Sun, Y.; Liu, Y.; Liu, L. Fixed-Time Synchronization for Fractional-Order Cellular Inertial Fuzzy Neural Networks with Mixed Time-Varying Delays. *Fractal Fract.* **2024**, *8*, 97. <https://doi.org/10.3390/fractalfract8020097>

Academic Editor: Jordan Hristov

Received: 2 January 2024

Revised: 30 January 2024

Accepted: 30 January 2024

Published: 4 February 2024



Copyright: © 2024 by the authors. Licensee MDPI, Basel, Switzerland. This article is an open access article distributed under the terms and conditions of the Creative Commons Attribution (CC BY) license (<https://creativecommons.org/licenses/by/4.0/>).

1. Introduction

In recent years, the CNNs conceptualized by Chua and Yang [1] have been widely used in many scientific and technological frontier fields, for example, associative memory, machine learning, pattern recognition, image processing, and combination optimization (see [2–5]). On the other hand, uncertainty or fuzziness cannot be ignored in the implementation of neural networks. Considering the existence of uncertainty or fuzziness, Yang and Yang [6] introduced a novel cellular neural network model known as the CFNN, which builds upon the foundation of traditional CNN models. The CFNN model differs from the conventional cellular neural network in that it incorporates both the product sum operation and the fuzzy logic operation between inputs and/or outputs. It was found that the fuzzy cellular neural network provides an effective example for pattern recognition and image processing. To date, the CFNN is still a hot research topic (see [7–10]).

In 1986, Babcock and Westervelt incorporated inductance into the Hopfield NNs to create INNs [11]. This modification was made to simulate the inertial characteristics of practical problems and phenomena. As we know, adding inertial terms may cause instability, bifurcation, chaos, and other complex dynamic behaviors. The introduction of inertial terms into the standard neural system has an obvious biological background. For example, the semicircular canal of mammals, the surface layer of hair cells, and the axons of squid can be simulated by equivalent circuits with inductance (see [12–14]). Therefore, the study of the dynamic behavior and synchronization control of INNs has an extensive practical background and significant application value.

As an extension and promotion of integral calculus (IC), FC can be traced back hundreds of years. Recently, FC has been widely used in mathematical modeling of economics, biology, physics, and other disciplines. Resulting from the infinite memory characteristics and genetic characteristics of fractional-order systems, an increasing number of scholars

have introduced fractional-order differential operators into neural network models; these models are commonly known as fractional-order neural network models (see [15–20]).

Because it takes time for neurons to process signals and transmit signals between them, time delay is inevitable, and time delay may directly lead to the oscillation or even instability of the NN system. On the other hand, because the mixed delay (MD) is more effective than single delay (SD) in complex network modeling, we usually consider the mixed delay in neural network system modeling [21].

Synchronization is a kind of dynamic behavior involving coupling neural network systems in order for them to reach the same state. Because of the wide application of synchronization in information science, security communication, and image processing, it has attracted the attention of many scholars [22–24]. At present, the synchronization of neural network systems can be primarily categorized into two types: infinite-time synchronization (IETS) and finite-time synchronization (FETS). IETS mainly includes exponential synchronization, quasi-synchronization, and asymptotic synchronization. FETS exhibits superior performance to IETS, thus enabling the system to achieve synchronization in a limited time. In practical applications, finite time synchronization is always desired, so it is imperative to investigate the FETS of NNs. Currently, research on delayed inertial neural networks primarily encompasses the following areas. Li et al. [25] focused on the asymptotic synchronization of INNs with a constant delay. Gu et al. [26] conducted a study on the asymptotic synchronization of Riemann–Liouville-type delayed IFNNs. Based on the pinning control method, Feng et al. [27] studied the exponential synchronization of hybrid delay INNs. Based on the intermittent control method, Tang et al. [28] studied the exponential synchronization of time-varying discrete and finite distribution delay inertial neural networks. Liang et al. [29] conducted an investigation into the exponential synchronization of Cohen–Grossberg NNs, taking into account inertial delays. Shi et al. [30] investigated the lag synchronization control and global exponential stability of inertial delay neural networks, employing the adaptive control theory as a foundational framework. Cui et al. [31] studied the FETS of INNs. Guo et al. [32] studied the FETS of delayed inertial memristor neural networks. Wei et al. [33] studied the finite time synchronization and fixed-time synchronization of time-varying delay inertial memristor neural networks. Chen et al. [34] discussed the FDTS control of discrete delay memristor NNs. Alimi et al. [35] studied the FETS and FDTS of INNs with multiple proportional delays. However, research on the FDTS control of delayed FCIFNNs is still rare, and it is important and meaningful to fill this gap.

To the best of our current knowledge, there is insufficient research on the FDTS control of FCIFNNs with MTD. This gap necessitates further investigation into this area. We primarily focus on the FDTS control issue for a class of FCIFNNs with MTD. The main innovation of this paper is shown in the following aspects.

- The FDTS problem of FCIFNNs with MTD is investigated for the first time. In practical applications, the performance of FDTS is better than asymptotic synchronization and FETS.
- By designing appropriate nonlinear controllers and selecting appropriate LF, some sufficient conditions are obtained to ensure that the RS and DS achieve FDTS.
- The cellular-inertial NN model proposed in this paper is more practical and general than the traditional neural network model because it contains four obvious characteristics, namely discontinuous activation function, mixed time-varying delay, fractional order, and fuzzy logic.
- New sufficient conditions are given by means of algebraic inequalities. Compared with matrix inequalities, algebraic inequalities are easy to realize and can avoid some complex calculations. The estimation of settlement time is straightforward. In addition, the estimated range of settlement time presented in this paper is more accurate and effective when compared to classical results.

- The efficacy of the proposed methods is demonstrated through numerical simulations. In addition, the developed fixed-time synchronization results are applied to the image encryption issue.

The remainder of this article is structured as follows. In Section 2, we present a network system model for FCIFNNs with mixed time-varying delays, establish relevant assumptions, provide lemmas, and define FDTS. The FDTS of the FCIFNNs is analyzed in Section 3. Section 4 presents two numerical examples that illustrate the effectiveness of the proposed control strategies. An application to image encryption is proposed to demonstrate the advantage of the obtained synchronization results in Section 5. In Section 6, the conclusion is revealed.

Notations: The symbols employed in this paper are as follows: R and R^+ are used to denote the set of real numbers and positive real numbers, respectively. R^n is employed to denote an n-dimensional vector space. $C^m[a, b]$ is employed to represent the set of continuous functions with m derivatives on the closed interval $[a, b]$. $C([-\tau, t_0], R^n)$ is used to denote the continuous functions mapping from $[-\tau, t_0]$ to R^n . \bar{co} is used to denote the convex closure of the set.

2. Problem Formulation and Preliminaries

Some related mathematical concepts are covered in this section, including the definition of fractional calculus, the solution of the fractional differential equation in Filippov’s sense [36,37], and the theory of fractional differential equations.

Definition 1 ([38]). *The fractional integral of order α is defined as follows*

$$I^{-\alpha}z(x) = \frac{1}{\Gamma(\alpha)} \int_{x_0}^x (x - s)^{\alpha-1}z(s)ds,$$

where $\alpha \in R^+, x > x_0$, and $\Gamma(\cdot)$ is the Gamma function.

Definition 2 ([38]). *The Caputo fractional derivative of order α is defined as follows*

$$D^\alpha z(x) = \frac{1}{\Gamma(m - \alpha)} \int_{x_0}^x (x - s)^{m-\alpha-1}z^{(m)}(s)ds,$$

where $m \in R^+$ and $m - 1 \leq \alpha < m$.

Remark 1. *Several definitions of fractional order $\alpha > 0$, for example, Caputo fractional derivatives, Riemann–Liouville fractional derivatives, Caputo–Febrizio fractional derivative are given. The Caputo definition is widely employed in engineering applications. This is because the Caputo definition takes into account the initial conditions for $f(t)$ and its integer order derivatives, which are physically meaningful in a conventional sense [39,40].*

In the paper, we investigate FCIFNNs with mixed delays as follows.

$$\begin{aligned}
 D^\alpha x_i(t) = & -a_i D^\beta x_i(t) - b_i x_i(t) + \sum_{w=1}^M c_{iw} h_w(x_w(t)) + \sum_{w=1}^M d_{iw} \int_{t-\tau_0(t)}^t h_w(x_w(s)) ds \\
 & + \sum_{w=1}^M g_{iw} v_w + \bigwedge_{w=1}^M T_{iw} v_w + \bigwedge_{w=1}^M \alpha_{iw} h_w(x_w(t - \tau_w(t))) + \bigvee_{w=1}^M S_{iw} v_w \\
 & + \bigvee_{w=1}^M \beta_{iw} h_w(x_w(t - \tau_w(t))) + I_i, i = 1, \dots, M,
 \end{aligned} \tag{1}$$

where $\beta \in [0, 1], \alpha \in (\beta, \beta + 1)$; $x_i(t)$ represents the state of the i th unit; a_i, b_i represent the passive decay rate of i th unit; c_{iw}, d_{iw} represent elements of feedback template, g_{iw} denotes the feedforward template; α_{iw}, β_{iw} are the elements of the fuzzy feedback MIN and MAX

template, respectively; T_{iw}, S_{iw} denote the element of the fuzzy feedforward MIN and MAX template, respectively; \wedge and \vee are the fuzzy AND and OR operations, respectively; v_i and I_i are input and bias of the i th neuron, respectively; h_i denotes discontinuous activation functions; and $\tau_0(t)$ and $\tau_w(t)$ represent the transmission delay.

The initial conditions of system (1) are given by

$$x_i(t) = \varphi_i(t), D^\beta x_i(t) = \psi_i(t), t \in [-\tau, t_0], \tag{2}$$

where $\tau = \max_{0 \leq w \leq M} \{ \sup_{t \in R^+} \tau_w(t) \}$, $\varphi_i(s), \psi_i(s)$ are initial functions.

Remark 2. If $\alpha = \beta$, system (1) degenerates into a general fractional system described as

$$\begin{aligned} D^\alpha x_i(t) = & -\frac{b_i}{a_i + 1} x_i(t) + \frac{1}{a_i + 1} \sum_{w=1}^M c_{iw} h_w(x_w(t)) + \frac{1}{a_i + 1} \sum_{w=1}^M d_{iw} \int_{t-\tau_0(t)}^t h_w(x_w(s)) ds \\ & + \frac{1}{a_i + 1} \sum_{w=1}^M g_{iw} v_w + \frac{1}{a_i + 1} \bigwedge_{w=1}^M T_{iw} v_w + \frac{1}{a_i + 1} \bigwedge_{w=1}^M \alpha_{iw} h_w(x_w(t - \tau_w(t))) \\ & + \frac{1}{a_i + 1} \bigvee_{w=1}^M S_{iw} v_w + \frac{1}{a_i + 1} \bigvee_{w=1}^M \beta_{iw} h_w(x_w(t - \tau_w(t))) + \frac{1}{a_i + 1} I_i, i = 1, \dots, M \end{aligned} \tag{3}$$

In this paper, we will be utilizing the following lemma and assumptions.

Assumption 1. There exist non-negative constants L_w and Q_w of the following.

$$|\lambda_w - \zeta_w| \leq L_w |x_w - y_w| + Q_w, \forall x_w, y_w \in R, w = 1, 2, \dots, M,$$

where $\lambda_w \in \overline{co}[h_w(x_w)]$ and $\zeta_w \in \overline{co}[h_w(y_w)]$.

Assumption 2. The activation function $h_i : R \rightarrow R$ is continuous except on a countable set $\{q_w^i\}$. Moreover, $h_i(q_w^{i-})$ and $h_i(q_w^{i+})$ exist. In addition, h_i exhibits at most a finite number of jump discontinuities.

To obtain the main results, we utilize the concept of Filippov solution, which originates from Filippov’s work on discontinuous systems (1).

Definition 3. The function $z = (z_1, z_2, \dots, z_M)^T$ is said to be a solution of mathematical model (1) on $[-\tau, T)$ if

- (i) $z = (z_1, z_2, \dots, z_M)^T$ is continuous in $[-\tau, T)$ and absolutely continuous in $[0, T)$ and
- (ii) there is a measurable function $\lambda = (\lambda_1, \lambda_2, \dots, \lambda_M)^T$ such that

$$\begin{aligned} D^\alpha x_i(t) = & -a_i D^\beta x_i(t) - b_i x_i(t) + \sum_{w=1}^M c_{iw} \lambda_w(t) + \sum_{w=1}^M d_{iw} \int_{t-\tau_0(t)}^t \lambda_w(s) ds \\ & + \sum_{w=1}^M g_{iw} v_w + \bigwedge_{w=1}^M T_{iw} v_w + \bigwedge_{w=1}^M \alpha_{iw} \lambda_w(t - \tau_w(t)) + \bigvee_{w=1}^M S_{iw} v_w \\ & + \bigvee_{w=1}^M \beta_{iw} \lambda_w(t - \tau_w(t)) + I_i, i = 1, \dots, M \end{aligned} \tag{4}$$

where $\lambda_w(t) \in \overline{co}[h_w(x_w(t))]$ for $t \in [-\tau, T]$.

Next, we perform the variable transformation as follows.

$$y_i(t) = D^\beta x_i(t) + \xi_i x_i(t)$$

Then, system (4) is re-described as follows.

$$\left\{ \begin{array}{l} D^\beta x_i(t) = -\zeta_i x_i(t) + y_i(t) \\ D^{\alpha-\beta} y_i(t) = -\theta_i y_i(t) + \delta_i x_i(t) + \sum_{w=1}^M c_{iw} \lambda_w(t) + \sum_{w=1}^M d_{iw} \int_{t-\tau_0(t)}^t \lambda_w(s) ds \\ \quad + \sum_{w=1}^M g_{iw} v_w + \bigwedge_{w=1}^M T_{iw} v_w + \bigwedge_{w=1}^M \alpha_{iw} \lambda_w(t - \tau_w(t)) + \bigvee_{w=1}^M S_{iw} v_w \\ \quad + \bigvee_{w=1}^M \beta_{iw} \lambda_w(t - \tau_w(t)) + \xi_i D^{\alpha-\beta} x_i(t) + I_i, i = 1, 2, \dots, M, \end{array} \right. \quad (5)$$

where $\theta_i = a_i$, $\delta_i = \zeta_i \theta_i - b_i$, and the initial values are re-expressed as follows.

$$\left\{ \begin{array}{l} x_i(t) = \varphi_i(t) \\ y_i(t) = \zeta_i \varphi_i(t) + \varphi_i(t) = \phi_i(t), t \in [-\tau, t_0]. \end{array} \right. \quad (6)$$

Now, we focus on system (5) as DS, and the corresponding RS is described below.

$$\left\{ \begin{array}{l} D^\beta p_i(t) = -\zeta_i p_i(t) + q_i(t) + u_i(t) \\ D^{\alpha-\beta} q_i(t) = -\theta_i q_i(t) + \delta_i p_i(t) + \sum_{w=1}^M c_{iw} \zeta_w(t) + \sum_{w=1}^M d_{iw} \int_{t-\tau_0(t)}^t \zeta_w(s) ds \\ \quad + \sum_{w=1}^M g_{iw} v_w + \bigwedge_{w=1}^M T_{iw} v_w + \bigwedge_{w=1}^M \alpha_{iw} \zeta_w(t - \tau_w(t)) + \bigvee_{w=1}^M S_{iw} v_w \\ \quad + \bigvee_{w=1}^M \beta_{iw} \zeta_w(t - \tau_w(t)) + \zeta_i D^{\alpha-\beta} p_i(t) + I_i + \tilde{u}_i(t), i = 1, 2, \dots, M, \end{array} \right. \quad (7)$$

where $p_i(t), q_i(t)$ represent the state variable, and $u_i(t), \tilde{u}_i(t)$ are control input. The synchronization error is defined as follows

$$\left\{ \begin{array}{l} \Delta_i(t) = p_i(t) - x_i(t) \\ \tilde{\Delta}_i(t) = q_i(t) - y_i(t) \end{array} \right.$$

The following error system is obtained.

$$\left\{ \begin{array}{l} D^\beta \Delta_i(t) = -\zeta_i \Delta_i(t) + \tilde{\Delta}_i(t) + u_i(t) \\ D^{\alpha-\beta} \tilde{\Delta}_i(t) = -\theta_i \tilde{\Delta}_i(t) + \delta_i \Delta_i(t) + \sum_{w=1}^M c_{iw} \zeta_w(t) - \sum_{w=1}^M c_{iw} \lambda_w(t) \\ \quad + \sum_{w=1}^M d_{iw} \int_{t-\tau_0(t)}^t \zeta_w(s) ds - \sum_{w=1}^M d_{iw} \int_{t-\tau_0(t)}^t \lambda_w(s) ds \\ \quad + \bigwedge_{w=1}^M \alpha_{iw} \zeta_w(t - \tau_w(t)) - \bigwedge_{w=1}^M \alpha_{iw} \lambda_w(t - \tau_w(t)) \\ \quad + \bigvee_{w=1}^M \beta_{iw} \zeta_w(t - \tau_w(t)) - \bigvee_{w=1}^M \beta_{iw} \lambda_w(t - \tau_w(t)) \\ \quad + \zeta_i D^{\alpha-\beta} e_i(t) + \tilde{u}_i(t), i = 1, 2, \dots, M. \end{array} \right. \quad (8)$$

Definition 4. The DS (5) and RS (7) are said to be synchronized within a fixed time T_{\max} if, with the controllers $u_w(t), \tilde{u}_w(t)$, there exists a settling time function $T(\Delta_0(t)) > t_0$ such that

$$\begin{cases} \lim_{t \rightarrow T(\Delta_0(t))} \|p_w(t) - x_w(t)\| = \lim_{t \rightarrow T(\Delta_0(t))} \|q_w(t) - y_w(t)\| = 0 \\ \|p_w(t) - x_w(t)\| = \|q_w(t) - y_w(t)\| = 0, \forall t > T(\Delta_0(t)) \\ T(\Delta_0(t)) \leq T_{\max}, \forall \Delta_0(t) \in C^m[-\tau, t_0], \end{cases}$$

where $w = 1, 2, \dots, M$, and $\|\cdot\|$ indicates the Euclidean norm.

Next, let us introduce some lemmas, which will be utilized in the following proof.

Lemma 1 ([41]). Let $x_w, y_w, \alpha_{iw}, \beta_{iw} \in R, h_w : R \rightarrow R$ be a continuous function for $i, w = 1, 2, \dots, M$. Then, we have

$$\begin{aligned} \left| \bigwedge_{w=1}^M \alpha_{iw} h_w(x_w) - \bigwedge_{w=1}^M \alpha_{iw} h_w(y_w) \right| &\leq \sum_{w=1}^M |\alpha_{iw}| |h_w(x_w) - h_w(y_w)| \\ \left| \bigvee_{w=1}^M \beta_{iw} h_w(x_w) - \bigvee_{w=1}^M \beta_{iw} h_w(y_w) \right| &\leq \sum_{w=1}^M |\beta_{iw}| |h_w(x_w) - h_w(y_w)| \end{aligned}$$

Lemma 2 ([41]). If $a_1, a_2, \dots, a_M \geq 0, \mu > 1, 0 < \nu \leq 1$, then

$$\sum_{w=1}^M a_w^\mu \geq M^{1-\mu} \left(\sum_{w=1}^M a_w \right)^\mu, \quad \sum_{w=1}^M a_w^\nu \geq \left(\sum_{w=1}^M a_w \right)^\nu$$

Lemma 3 ([42]). Suppose that there exist constants $a, b, \mu, q > 0, \mu q > 1$ and a positive unbounded function $V(x(t)) : R^n \rightarrow R^+ \cup \{0\}$ such that

$$\dot{V}(x(t)) \leq - \left(a V^\mu(x(t)) + b \right)^q, \forall x(t) \in R^n \setminus \{0\}$$

Then, we have $V(x(t)) = 0, t \geq T(x(t_0))$ with the settling time bounded by

$$T(x(t_0)) \leq T_{\max} = \frac{1}{b^q} \left(\frac{b}{a} \right)^{\frac{1}{\mu}} \left(1 + \frac{1}{\mu q - 1} \right)$$

Lemma 4 ([43]). Suppose that $x(t) \in C^1[0, T]$. Then,

$$D^{\beta_1} D^{\beta_2} x(t) = D^{\beta_1 + \beta_2} x(t),$$

where $\beta_1, \beta_2 > 0$ and $\beta_1 + \beta_2 \leq 1; T$ is a positive constant.

3. FDTS of the Drive FCIFNNs and Response FCIFNNs

In this section, we propose novel criteria for achieving FDTS between DS and RS. According to Definition 4, the fixed time synchronization problem between the driving system (5) and the response system (7) can be equivalent to the fixed time stability problem of the error system (8). To achieve this goal, the designed controller is as follows.

$$\begin{cases} u_i(t) = -k_i \Delta_i(t) - \text{sign}(\Delta_i(t)) \left(\gamma_i + c \left(D^{\beta-1} |\Delta_i(t)| \right)^\mu + \omega_i |\Delta_i(t - \tau_i(t))| \right) \\ \tilde{u}_i(t) = -\eta_{i1} \tilde{\Delta}_i(t) - \text{sign}(\tilde{\Delta}_i(t)) \left(\eta_{i2} + c \left(D^{\alpha-\beta-1} |\tilde{\Delta}_i(t)| \right)^\mu \right) \\ - \sum_{w=1}^M d_{iw} \int_{t-\tau_0(t)}^t \zeta_w(s) ds + \sum_{w=1}^M d_{iw} \int_{t-\tau_0(t)}^t \lambda_w(s) ds \\ - \zeta_i D^{\alpha-\beta} \Delta_i(t), i = 1, 2, \dots, M, \end{cases} \quad (9)$$

where $0 < \mu < 1, c > 0$, and $k_i, \gamma_i, \omega_i, \eta_{i1}$, and η_{i2} are the control parameters.

Theorem 1. Under Assumptions 1 and 2 and with controller (9), the DS (5) and RS (7) can achieve FDTs if the following conditions are met.

$$\begin{cases} \eta_{i1} \geq 1 - \theta_i \\ \eta_{i2} \geq \sum_{w=1}^M \left(|\alpha_{iw}| + |\beta_{iw}| + |c_{iw}| \right) Q_w \\ k_i \geq \sum_{w=1}^M |c_{wi}| L_i + \delta_i + \zeta_i \\ \omega_i \geq \sum_{w=1}^M \left(|\alpha_{iw}| + |\beta_{iw}| \right) L_i \end{cases} \quad (10)$$

for $i = 1, 2, \dots, M$. Furthermore, the T_{\max} can be calculated using Equation (11).

$$T_{\max} = \frac{1}{\varpi} \left(\frac{\varpi}{\rho} \right)^{\frac{1}{\mu}} \left(1 + \frac{1}{\mu - 1} \right), \quad (11)$$

where $\rho = cM^{1-\mu}$ and $\varpi = \sum_{i=1}^M \gamma_i$.

Proof. The LF is selected as follows:

$$V(t) = \sum_{i=1}^M D^{\beta-1} |\Delta_i(t)| + \sum_{i=1}^M D^{\alpha-\beta-1} |\tilde{\Delta}_i(t)| \quad (12)$$

Based on Lemma 4, we derive the following results.

$$\begin{aligned} \dot{V}(t) &= \left(\sum_{i=1}^M D^{\beta-1} |\Delta_i(t)| \right)' + \left(\sum_{i=1}^M D^{\alpha-\beta-1} |\tilde{\Delta}_i(t)| \right)' \\ &= D^\beta D^{1-\beta} \left(\sum_{i=1}^M D^{\beta-1} |\Delta_i(t)| \right) + D^{\alpha-\beta} D^{1-\beta+\beta} \left(\sum_{i=1}^M D^{\alpha-\beta-1} |\tilde{\Delta}_i(t)| \right) \\ &= D^\beta \left(\sum_{i=1}^M D^{1-\beta} D^{\beta-1} |\Delta_i(t)| \right) + D^{\alpha-\beta} \left(\sum_{i=1}^M D^{1-\beta+\beta} D^{\alpha-\beta-1} |\tilde{\Delta}_i(t)| \right) \\ &= \sum_{i=1}^M D^\beta |\Delta_i(t)| + \sum_{i=1}^M D^{\alpha-\beta} |\tilde{\Delta}_i(t)| \\ &\leq \sum_{i=1}^M \text{sign}(\Delta_i(t)) D^\beta \Delta_i(t) + \sum_{i=1}^M \text{sign}(\tilde{\Delta}_i(t)) D^{\alpha-\beta} \tilde{\Delta}_i(t) \end{aligned}$$

which yields that

$$\begin{aligned} \dot{V}(t) \leq & \sum_{i=1}^M \text{sign}(\Delta_i(t)) \left(-\xi_i \Delta_i(t) + \tilde{\Delta}_i(t) + u_i(t) \right) + \sum_{i=1}^M \text{sign}(\tilde{\Delta}_i(t)) \left(-\theta_i \tilde{\Delta}_i(t) + \delta_i \Delta_i(t) \right) \\ & + \sum_{w=1}^M c_{iw} \zeta_w(t) - \sum_{w=1}^M c_{iw} \lambda_w(t) + \sum_{w=1}^M d_{iw} \int_{t-\tau_0(t)}^t \zeta_w(s) ds - \sum_{w=1}^M d_{iw} \int_{t-\tau_0(t)}^t \lambda_w(s) ds \\ & + \bigwedge_{w=1}^M \alpha_{iw} \zeta_w(t - \tau_w(t)) - \bigwedge_{w=1}^M \alpha_{iw} \lambda_w(t - \tau_w(t)) \\ & + \bigvee_{w=1}^M \beta_{iw} \zeta_w(t - \tau_w(t)) - \bigvee_{w=1}^M \beta_{iw} \lambda_w(t - \tau_w(t)) \\ & + \xi_i D^{\alpha-\beta} \Delta_i(t) + \tilde{u}_i(t) \end{aligned}$$

Substituting (9) into above formula, we obtain

$$\begin{aligned} \dot{V}(t) \leq & \sum_{i=1}^M \text{sign}(\Delta_i(t)) \left(-\xi_i \Delta_i(t) + \tilde{\Delta}_i(t) - k_i \Delta_i(t) - \text{sign}(\Delta_i(t)) (\gamma_i + c(D^{\beta-1} |\Delta_i(t)|)^\mu) \right. \\ & \left. + \omega_i |\Delta_i(t - \tau_i(t))| \right) + \sum_{i=1}^M \text{sign}(\tilde{\Delta}_i(t)) \left(-\theta_i \tilde{\Delta}_i(t) + \delta_i \Delta_i(t) + \sum_{w=1}^M c_{iw} \zeta_w(t) \right. \\ & - \sum_{w=1}^M c_{iw} \lambda_w(t) + \sum_{w=1}^M d_{iw} \int_{t-\tau_0(t)}^t \zeta_w(s) ds - \sum_{w=1}^M d_{iw} \int_{t-\tau_0(t)}^t \lambda_w(s) ds \\ & + \bigwedge_{w=1}^M \alpha_{iw} \zeta_w(t - \tau_w(t)) - \bigwedge_{w=1}^M \alpha_{iw} \lambda_w(t - \tau_w(t)) \\ & + \bigvee_{w=1}^M \beta_{iw} \zeta_w(t - \tau_w(t)) - \bigvee_{w=1}^M \beta_{iw} \lambda_w(t - \tau_w(t)) \\ & + \xi_i D^{\alpha-\beta} \Delta_i(t) - \eta_{i1} \tilde{\Delta}_i(t) - \text{sign}(\tilde{\Delta}_i(t)) (\eta_{i2} \\ & + c(D^{\alpha-\beta-1} |\tilde{\Delta}_i(t)|)^\mu) - \sum_{w=1}^M d_{iw} \int_{t-\tau_0(t)}^t \zeta_w(s) ds \\ & \left. + \sum_{w=1}^M d_{iw} \int_{t-\tau_0(t)}^t \lambda_w(s) ds - \xi_i D^{\alpha-\beta} \Delta_i(t) \right) \end{aligned}$$

which yields that

$$\begin{aligned} \dot{V}(t) \leq & \sum_{i=1}^M [-\xi_i - k_i + \delta_i] |\Delta_i(t)| + \sum_{i=1}^M [1 + \theta_i - \eta_{i1}] |\tilde{\Delta}_i(t)| - \sum_{i=1}^M \omega_i |\Delta_i(t - \tau_i(t))| \\ & - \sum_{i=1}^M c(D^{\beta-1} |\Delta_i(t)|)^\mu - \sum_{i=1}^M (\eta_{i2} + c(D^{\alpha-\beta-1} |\tilde{\Delta}_i(t)|)^\mu) \\ & + \sum_{i=1}^M \left| \bigwedge_{w=1}^M \alpha_{iw} \zeta_w(t - \tau_w(t)) - \bigwedge_{w=1}^M \alpha_{iw} \lambda_w(t - \tau_w(t)) \right| \\ & + \sum_{i=1}^M \left| \bigvee_{w=1}^M \beta_{iw} \zeta_w(t - \tau_w(t)) - \bigvee_{w=1}^M \beta_{iw} \lambda_w(t - \tau_w(t)) \right| \\ & + \sum_{i=1}^M \sum_{w=1}^M |c_{iw}| |\zeta_w(t) - \lambda_w(t)| - \sum_{i=1}^M \gamma_i \end{aligned}$$

Based on Assumption 1, we have

$$\begin{aligned} \sum_{i=1}^M \sum_{w=1}^M |c_{iw}| |\zeta_w(t) - \lambda_w(t)| &\leq \sum_{i=1}^M \sum_{w=1}^M |c_{iw}| (L_i |\Delta_w(t)| + Q_i) \\ &= \sum_{i=1}^M \sum_{w=1}^M |c_{wi}| (L_i |\Delta_i(t)| + Q_i) \end{aligned}$$

Using Assumption 1 and Lemma 1, we can easily obtain the desired result.

$$\begin{aligned} \left| \bigwedge_{w=1}^M \alpha_{iw} \zeta_w(t - \tau_w(t)) - \bigwedge_{w=1}^M \alpha_{iw} \lambda_w(t - \tau_w(t)) \right| &\leq \sum_{w=1}^M |\alpha_{iw}| |\zeta_w(t - \tau_w(t)) - \lambda_w(t - \tau_w(t))| \\ &\leq \sum_{w=1}^M |\alpha_{wi}| (L_i |\Delta_w(t - \tau_w(t))| + Q_i) \end{aligned}$$

Similarly,

$$\begin{aligned} \left| \bigvee_{w=1}^M \beta_{iw} \zeta_w(t - \tau_w(t)) - \bigvee_{w=1}^M \beta_{iw} \lambda_w(t - \tau_w(t)) \right| &\leq \sum_{w=1}^M |\beta_{iw}| |\zeta_w(t - \tau_w(t)) - \lambda_w(t - \tau_w(t))| \\ &\leq \sum_{w=1}^M |\beta_{wi}| (L_i |\Delta_w(t - \tau_w(t))| + Q_i) \end{aligned}$$

Utilizing the aforementioned inequality, we can derive

$$\begin{aligned} \dot{V}(t) &\leq \sum_{i=1}^M [-\zeta_i - k_i + \delta_i + \sum_{w=1}^M |c_{wi} L_i| |\Delta_i(t)| + \sum_{i=1}^M [1 + \theta_i - \eta_{i1}] |\tilde{\Delta}_i(t)|] \\ &\quad + \sum_{i=1}^M \left(\sum_{w=1}^M (|\alpha_{wi}| + |\beta_{wi}|) L_i - \omega_i \right) |\Delta_i(t - \tau_i(t))| \\ &\quad + \sum_{i=1}^M \left(\sum_{w=1}^M (|\alpha_{iw}| + |\beta_{iw}| + |c_{iw}|) Q_i - \eta_{i2} \right) - \sum_{i=1}^M \gamma_i \\ &\quad - \sum_{i=1}^M c \left(D^{\beta-1} |\Delta_i(t)| \right)^\mu - \sum_{i=1}^M c \left(D^{\alpha-\beta-1} |\tilde{\Delta}_i(t)| \right)^\mu \end{aligned}$$

From (10) and Lemma 2, we obtain

$$\begin{aligned} \dot{V}(t) &\leq - \sum_{i=1}^M c \left(D^{\beta-1} |\Delta_i(t)| \right)^\mu - \sum_{i=1}^M c \left(D^{\alpha-\beta-1} |\tilde{\Delta}_i(t)| \right)^\mu - \sum_{i=1}^M \gamma_i \\ &\leq -cM^{1-\mu} \left(\sum_{i=1}^M D^{\beta-1} |\Delta_i(t)| + \sum_{i=1}^M D^{\alpha-\beta-1} |\tilde{\Delta}_i(t)| \right)^\mu - \sum_{i=1}^M \gamma_i \\ &= -\rho V^\mu(t) - \omega, \end{aligned}$$

where $\rho = cM^{1-\mu}$ and $\omega = \sum_{i=1}^M \gamma_i$. Therefore, the FDTS between the DS (5) and RS (7) can be achieved by Lemma 3. In addition, the settling time T_{\max} can be calculated by (11). \square

Remark 3. In Theorem 1, the FDTS of FCI-FNNs with MTD is achieved by designing an appropriate controller. However, $u_i(t)$ and $\tilde{u}_i(t)$ are difficult to adapt. The two distributed time-delay terms in $\tilde{u}_i(t)$ satisfy some special conditions. In order to enhance the feasibility of our results, we will refine the applicable laws $\tilde{u}_i(t)$.

The state feedback controller is designed as follows.

$$\begin{cases} u_i(t) = -k_i \Delta_i(t) - \text{sign}(\Delta_i(t)) \left(\gamma_i + c \left(D^{\beta-1} |\Delta_i(t)| \right)^\mu + \omega_i |\Delta_i(t - \tau_i(t))| \right) \\ \tilde{u}_i(t) = -\eta_{i1} \tilde{\Delta}_i(t) - \text{sign}(\tilde{\Delta}_i(t)) \left(\eta_{i2} + c \left(D^{\alpha-\beta-1} |\tilde{\Delta}_i(t)| \right)^\mu \right) \\ - \text{sign}(\tilde{\Delta}_i(t)) \sum_{w=1}^M L_i |d_{iw}| \int_{t-\tau_0(t)}^t |\Delta_w(s)| ds - \zeta_i D^{\alpha-\beta} \Delta_i(t), i = 1, 2, \dots, M, \end{cases} \quad (13)$$

where $0 < \mu < 1, c > 0$. The control parameters are denoted by $k_i, \gamma_i, \omega_i, \eta_{i1}, \eta_{i2}$. Consequently, we establish the following theorem.

Theorem 2. Under Assumptions 1 and 2 and with controller (9), (5) and (7) can achieve fixed-time synchronization if the aforementioned conditions are met.

$$\begin{cases} \eta_{i1} \geq 1 - \theta_i \\ \eta_{i2} \geq \sum_{w=1}^M \left(|\alpha_{iw}| + |\beta_{iw}| + |c_{iw}| + \tau |d_{iw}| \right) Q_i \\ k_i \geq \sum_{w=1}^M |c_{wi}| L_i + \delta_i + \zeta_i \\ \omega_i \geq \sum_{w=1}^M \left(|\alpha_{iw}| + |\beta_{iw}| \right) L_i \end{cases} \quad (14)$$

for $i = 1, 2, \dots, M$. Furthermore, the settling time T_{\max} can be calculated by the following formula

$$T_{\max} = \frac{1}{\varpi} \left(\frac{\varpi}{\rho} \right)^{\frac{1}{\mu}} \left(1 + \frac{1}{\mu - 1} \right), \quad (15)$$

where $\rho = cM^{1-\mu}$ and $\varpi = \sum_{i=1}^M \gamma_i$.

Proof. The proof follows a similar process as Theorem 1, so we will not provide a detailed proof here. \square

4. Numerical Simulations

In this section, two numerical examples are presented to validate the effectiveness of Theorems 1 and 2.

Example 1. Considering the following FCIFNNs with the drive system

$$\begin{cases} D^\beta x_i(t) = -\zeta_i x_i(t) + y_i(t) \\ D^{\alpha-\beta} y_i(t) = -\theta_i y_i(t) + \delta_i x_i(t) + \sum_{w=1}^2 c_{iw} \lambda_w(t) + \sum_{w=1}^2 d_{iw} \int_{t-\tau_0(t)}^t \lambda_w(s) ds \\ + \sum_{w=1}^2 g_{iw} v_w + \sum_{w=1}^2 T_{iw} v_w + \sum_{w=1}^2 \alpha_{iw} \lambda_w(t - \tau_w(t)) + \sum_{w=1}^2 S_{iw} v_w \\ + \sum_{w=1}^m \beta_{iw} \lambda_w(t - \tau_w(t)) + \zeta_i D^{\alpha-\beta} x_i(t) + I_i, i = 1, 2, \end{cases} \quad (16)$$

The following is a description of the response system.

$$\left\{ \begin{array}{l} D^\beta p_i(t) = -\zeta_i p_i(t) + q_i(t) + u_i(t) \\ D^{\alpha-\beta} q_i(t) = -\theta_i q_i(t) + \delta_i p_i(t) + \sum_{w=1}^2 c_{iw} \zeta_w(t) + \sum_{w=1}^2 d_{iw} \int_{t-\tau_0(t)}^t \zeta_w(s) ds \\ \quad + \sum_{w=1}^2 g_{iw} v_w + \bigwedge_{w=1}^2 T_{iw} v_w + \bigwedge_{w=1}^2 \alpha_{iw} \zeta_w(t - \tau_w(t)) + \bigvee_{w=1}^2 S_{iw} v_w \\ \quad + \bigvee_{w=1}^2 \beta_{iw} \zeta_w(t - \tau_w(t)) + \xi_i D^{\alpha-\beta} p_i(t) + I_i + \tilde{u}_i(t), i = 1, 2, \end{array} \right. \quad (17)$$

where

$$h_i(f) = \begin{cases} \tanh(f) + 0.8, & f \geq 0, \\ \tanh(f) - 0.8, & f \leq 0, \end{cases} \quad i = 1, 2.$$

It is not difficult to verify that the activation functions meet Assumptions 1 and 2 with $L_i = 4, Q_i = 5, i = 1, 2$. The system parameters are given as follows.

$$\left\{ \begin{array}{l} \alpha = 0.95, \beta = 0.85; \\ a_1 = 3, a_2 = 2, b_1 = b_2 = 1, \zeta_1 = 0.2, \zeta_2 = 0.1; \\ c_{11} = c_{21} = -0.1, c_{12} = 0.3, c_{22} = 0.2 \\ \alpha_{11} = \alpha_{12} = \alpha_{21} = \alpha_{22} = -0.01; \\ \beta_{11} = \beta_{12} = \beta_{21} = \beta_{22} = 0.1; \\ d_{11} = d_{12} = d_{21} = d_{22} = 0; \\ I_1 = I_2 = 0, \tau_i(t) = 0.7 + 0.3 \cos(2t), i = 0, 1, 2. \end{array} \right.$$

The following controller is suggested

$$\left\{ \begin{array}{l} u_i(t) = -k_i \Delta_i(t) - \text{sign}(\Delta_i(t)) \left(\gamma_i + c \left(D^{\beta-1} |\Delta_i(t)| \right)^\mu + \omega_i |\Delta_i(t - \tau_i(t))| \right) \\ \tilde{u}_i(t) = -\eta_{i1} \tilde{\Delta}_i(t) - \text{sign}(\tilde{\Delta}_i(t)) \left(\eta_{i2} + c \left(D^{\alpha-\beta-1} |\tilde{\Delta}_i(t)| \right)^\mu \right) \\ \quad - \sum_{w=1}^2 d_{iw} \int_{t-\tau_0(t)}^t \zeta_w(s) ds + \sum_{w=1}^2 d_{iw} \int_{t-\tau_0(t)}^t \lambda_w(s) ds \\ \quad - \zeta_i D^{\alpha-\beta} \Delta_i(t), i = 1, 2, \end{array} \right. \quad (18)$$

The controller parameter values chosen are as follows.

$$\left\{ \begin{array}{l} k_1 = k_2 = 2, \omega_1 = \omega_2 = 1, c = 4; \\ \eta_{11} = \eta_{21} = 2, \gamma_1 = \gamma_2 = 2, \mu = 1.5. \end{array} \right.$$

The initial values are chosen as

$$\left\{ \begin{array}{l} x_1(t) = 2, x_2(t) = 3, p_1(t) = 4, p_2(t) = 1; \\ y_1(t) = 4, y_2(t) = 1, q_1(t) = 2, q_2(t) = 4. \end{array} \right.$$

It is straightforward to confirm that all the conditions of Theorem 1 are met. Thus, RS (17) can synchronize with the DS (16) in a fixed time. In addition, according to Theorem 1, T_{\max} can be computed using the following formula.

$$T_{\max} = \frac{1}{\varpi} \left(\frac{\varpi}{\rho} \right)^{\frac{1}{\mu}} \left(1 + \frac{1}{\mu - 1} \right) = 0.9449$$

The simulation results are depicted in Figures 1–5. The simulation results confirm the validity of the main findings regarding fixed-time synchronization established in this paper.

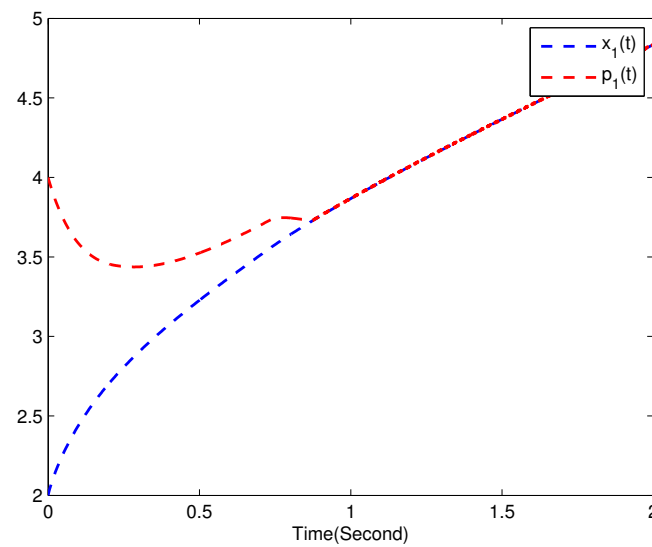


Figure 1. State trajectories of $x_1(t)$ and $p_1(t)$.

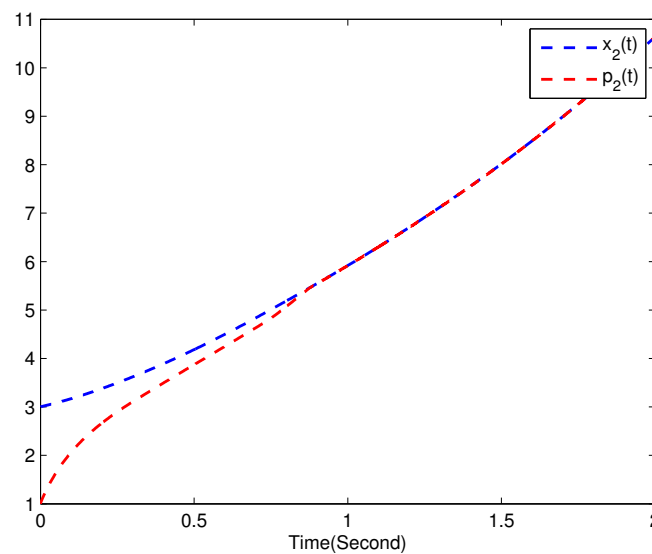


Figure 2. State trajectories of $x_2(t)$ and $p_2(t)$.

Example 2. Considering the following FCIFNNs with the drive system

$$\left\{ \begin{array}{l} D^\beta x_i(t) = -\xi_i x_i(t) + y_i(t) \\ D^{\alpha-\beta} y_i(t) = -\theta_i y_i(t) + \delta_i x_i(t) + \sum_{w=1}^2 c_{iw} \lambda_w(t) + \sum_{w=1}^2 d_{iw} \int_{t-\tau_0(t)}^t \lambda_w(s) ds \\ \quad + \sum_{w=1}^2 g_{iw} v_w + \bigwedge_{w=1}^2 T_{iw} v_w + \bigwedge_{w=1}^2 \alpha_{iw} \lambda_w(t - \tau_w(t)) + \bigvee_{w=1}^2 S_{iw} v_w \\ \quad + \bigvee_{w=1}^2 \beta_{iw} \lambda_w(t - \tau_w(t)) + \xi_i D^{\alpha-\beta} x_i(t) + I_i, i = 1, 2, \end{array} \right. \quad (19)$$

and the corresponding response system described as

$$\left\{ \begin{array}{l} D^\beta p_i(t) = -\xi_i p_i(t) + q_i(t) + u_i(t) \\ D^{\alpha-\beta} q_i(t) = -\theta_i q_i(t) + \delta_i p_i(t) + \sum_{w=1}^2 c_{iw} \zeta_w(t) + \sum_{w=1}^2 d_{iw} \int_{t-\tau_0(t)}^t \zeta_w(s) ds \\ \quad + \sum_{w=1}^2 g_{iw} v_w + \bigwedge_{w=1}^2 T_{iw} v_w + \bigwedge_{w=1}^2 \alpha_{iw} \zeta_w(t - \tau_w(t)) + \bigvee_{w=1}^2 S_{iw} v_w \\ \quad + \bigvee_{w=1}^2 \beta_{iw} \zeta_w(t - \tau_w(t)) + \xi_i D^{\alpha-\beta} p_i(t) + I_i + \tilde{u}_i(t), i = 1, 2, \end{array} \right. \quad (20)$$

where

$$h_i(f) = \begin{cases} \tanh(f) + 0.5, & f \geq 0, \\ \tanh(f) - 0.5, & f \leq 0, \end{cases} \quad i = 1, 2.$$

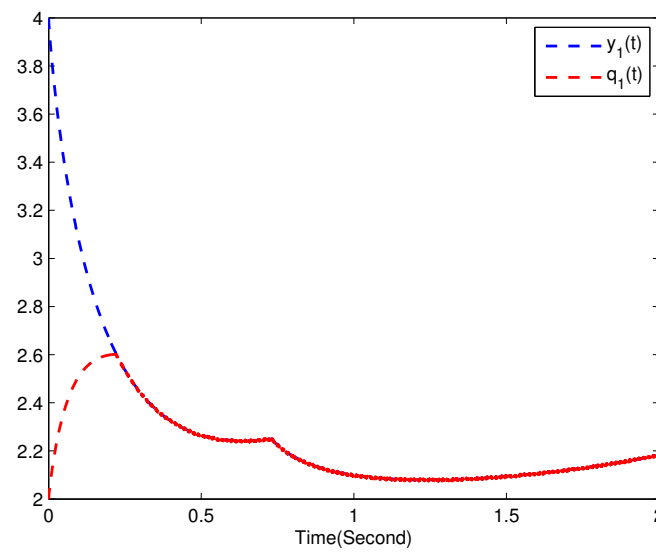


Figure 3. State trajectories of $y_1(t)$ and $q_1(t)$.

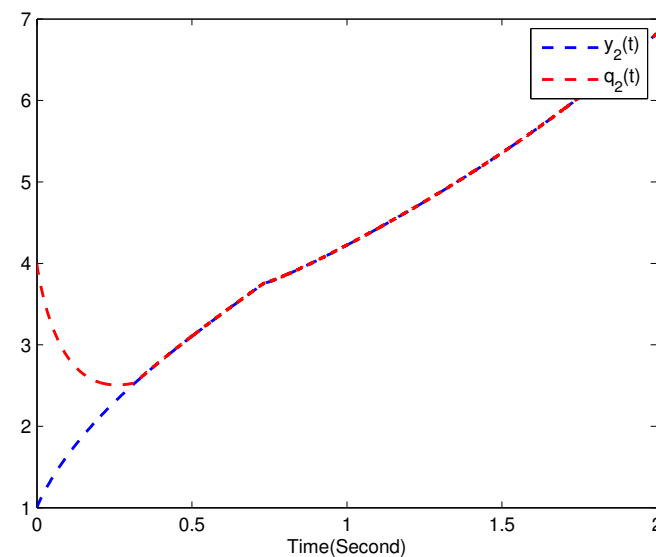


Figure 4. State trajectories of $y_2(t)$ and $q_2(t)$.

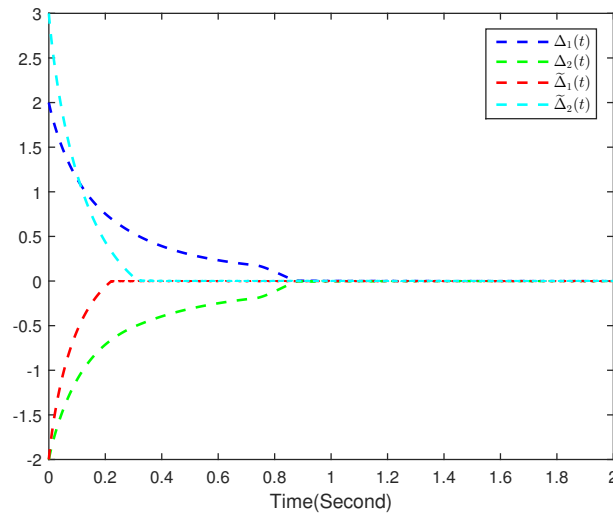


Figure 5. Synchronization errors of $\Delta_1(t), \Delta_2(t), \tilde{\Delta}_1(t), \tilde{\Delta}_2(t)$ between systems (16) and (17).

It is not difficult to verify that the activation functions meet Assumptions 1 and 2 with $L_i = Q_i = 1, i = 1, 2$. The system parameters are chosen as follows.

$$\begin{cases} \alpha = 0.90, \beta = 0.45; \\ a_1 = a_2 = 3, b_1 = b_2 = 1, \zeta_1 = -0.1, \zeta_2 = -0.2; \\ c_{11} = c_{21} = -0.2, c_{12} = c_{22} = 0.2 \\ \alpha_{11} = \alpha_{12} = \alpha_{21} = \alpha_{22} = -0.1; \\ \beta_{11} = \beta_{12} = \beta_{21} = \beta_{22} = 0.5; \\ d_{11} = d_{21} = -1, d_{12} = d_{22} = 1; \\ I_1 = I_2 = 0, \tau_i(t) = 0.7 + 0.3 \cos(2t), i = 0, 1, 2. \end{cases}$$

The following controller is suggested

$$\begin{cases} u_i(t) = -k_i \Delta_i(t) - \text{sign}(\Delta_i(t)) \left(\gamma_i + c \left(D^{\beta-1} |\Delta_i(t)| \right)^\mu + \omega_i |\Delta_i(t - \tau_i(t))| \right) \\ \tilde{u}_i(t) = -\eta_{i1} \tilde{\Delta}_i(t) - \text{sign}(\tilde{\Delta}_i(t)) \left(\eta_{i2} + c \left(D^{\alpha-\beta-1} |\tilde{\Delta}_i(t)| \right)^\mu \right) \\ - \text{sign}(\tilde{\Delta}_i(t)) \sum_{w=1}^2 L_w |d_{iw}| \int_{t-\tau_0(t)}^t |\Delta_w(s)| ds - \zeta_i D^{\alpha-\beta} \Delta_i(t), i = 1, 2. \end{cases} \tag{21}$$

where

$$\begin{cases} k_1 = 2, k_2 = 2, \omega_1 = 1.2, \omega_2 = 0.8, c = 16; \\ \eta_{11} = 2, \eta_{21} = 3, \gamma_1 = 2, \gamma_2 = 3, \mu = 1.5. \end{cases}$$

The initial values are chosen as

$$\begin{cases} x_1(t) = 5, x_2(t) = 3, p_1(t) = -5, p_2(t) = -2; \\ y_1(t) = -4, y_2(t) = 3, q_1(t) = 2, q_2(t) = 6. \end{cases}$$

It is easy to verify that all the conditions of Theorem 2 are satisfied. Thus, RS (20) can synchronize with the DS (19) in a fixed time. Furthermore, according to Theorem 2, T_{\max} can be computed using the following formula.

$$T_{\max} = \frac{1}{\omega} \left(\frac{\omega}{\rho} \right)^{\frac{1}{\mu}} \left(1 + \frac{1}{\mu - 1} \right) = 0.3481$$

The simulation results are shown in Figures 6–10. The simulation implies that the main result of FDTS established in the present paper is correct.

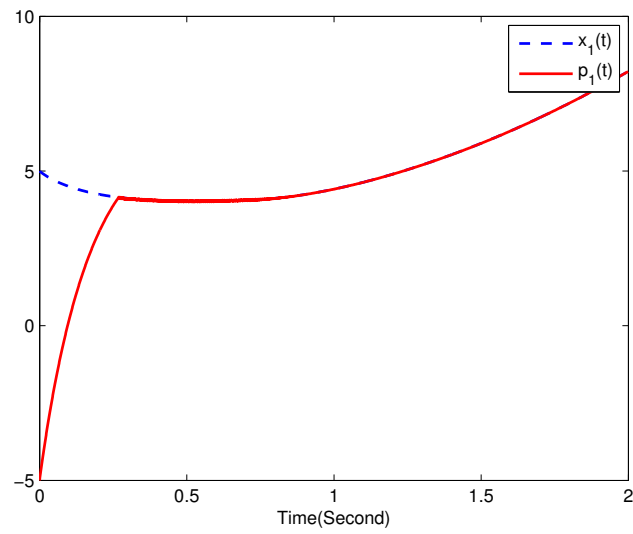


Figure 6. State trajectories of $x_1(t)$ and $p_1(t)$.

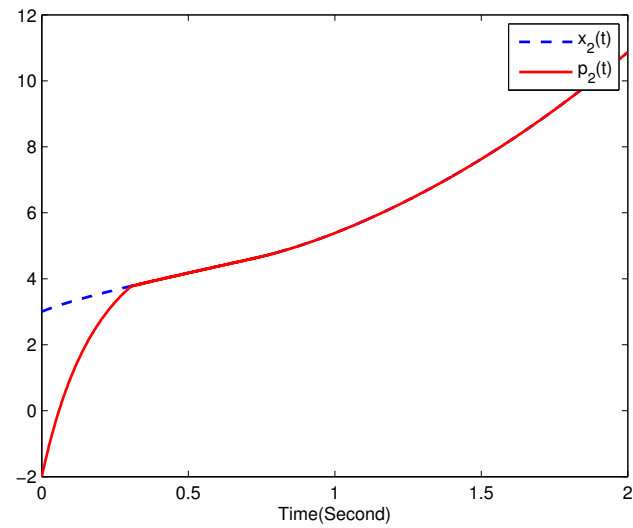


Figure 7. State trajectories of $x_2(t)$ and $p_2(t)$.

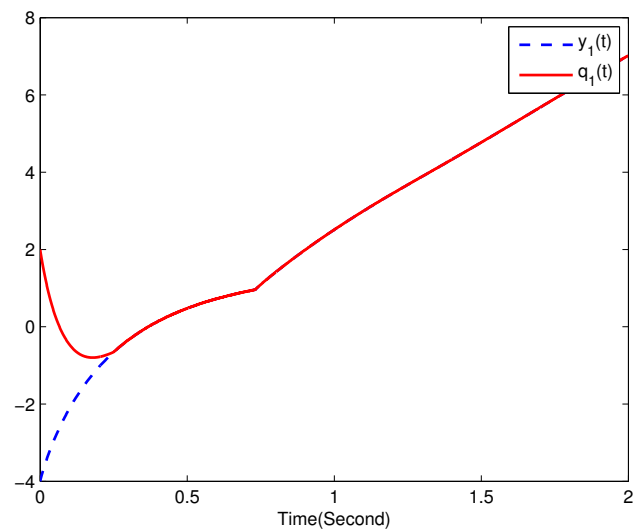


Figure 8. State trajectories of $y_1(t)$ and $q_1(t)$.

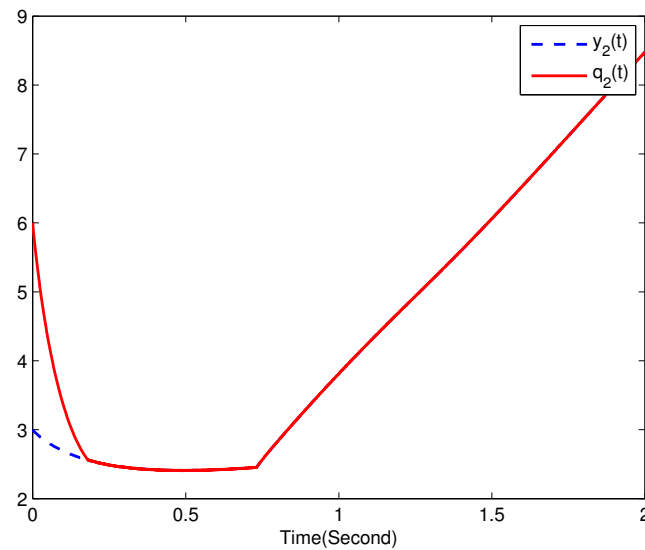


Figure 9. State trajectories of $y_2(t)$ and $q_2(t)$.

The theoretical results are consistent with the simulation results, indicating that the proposed method is effective.

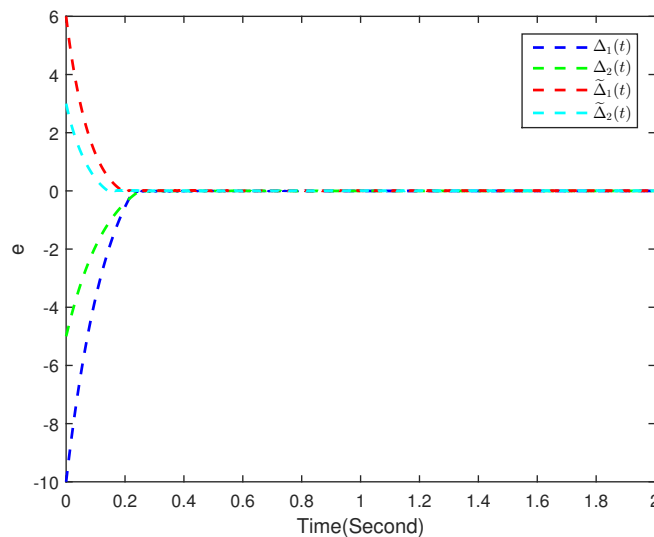


Figure 10. Synchronization errors of $\Delta_1(t)$, $\Delta_2(t)$, $\tilde{\Delta}_1(t)$, $\tilde{\Delta}_2(t)$ between systems (19) and (20).

5. Application to Image Encryption

In this section, the developed fixed-time synchronization result of FCIFNNs with MTD derived from Theorem 1 is applied to the image encryption issue. The same parameters in Example 1 are chosen. For a color picture Pic of size $m \times n \times 3$, the encryption algorithms proposed in [44,45] are used. To demonstrate the effectiveness of the encryption algorithm, a color picture named Lina is applied to show the validity of the presented encryption algorithm; see Figure 11.

The histograms of red, green, and blue channels for the original Lina image and the encrypted Lina image are illustrated in Figure 12. From Figure 11, it can be seen that through the proposed encryption algorithm, the encrypted image can be successfully decrypted after the system reaches synchronization. In addition, the histogram of the encrypted image in Figure 12 shows almost uniform distribution. The results indicate that encryption algorithms enhance the randomness of the color distribution in the original image, thereby improving the security of the encryption algorithm.

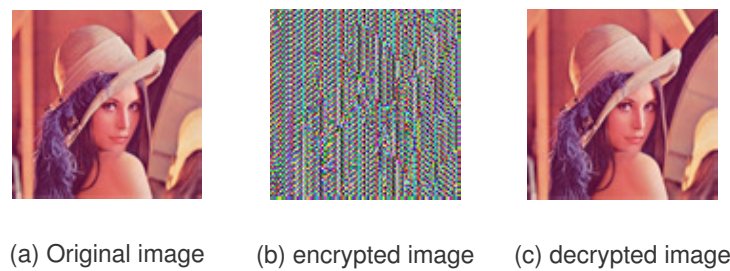


Figure 11. Original, encrypted, and decrypted images of Lena with the encryption algorithm.

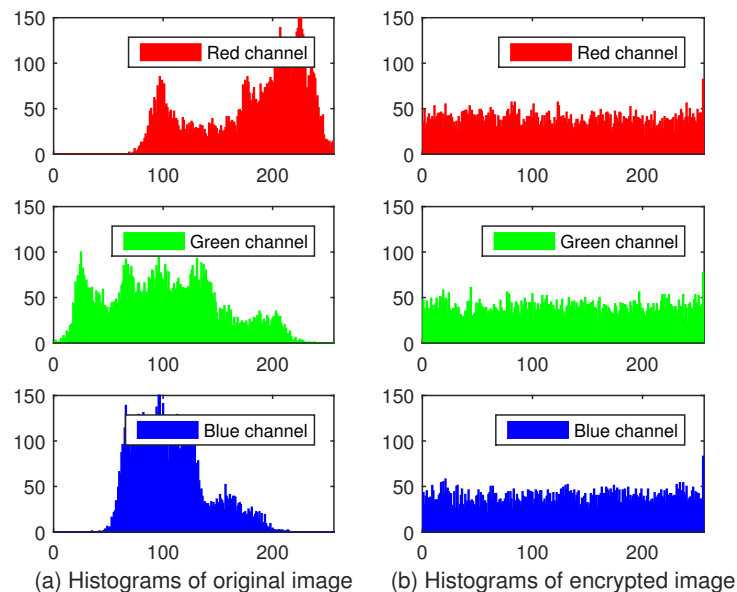


Figure 12. Histograms of the original Lena and the encrypted Lena.

6. Conclusions

This paper investigates the FDTS problem for a class of FCIFNNs with MTD. Using the theory of finite-time stability and Lyapunov functional analysis techniques, we have derived some new sufficient conditions for FDTS in drive–response systems. Finally, we present two simulation examples and their practical application in image encryption, demonstrating the effectiveness of the proposed approach. In the future, we plan to extend the results of this paper to more general neural networks and design more effective control strategies. This is a challenging topic.

Author Contributions: Conceptualization, Y.S.; methodology, Y.S. and Y.L.; writing—original draft preparation, Y.S.; writing—review and editing, Y.L.; numerical simulation, L.L. All authors have read and agreed to the published version of the manuscript.

Funding: This work is partially supported by the Program for Innovative Research Team in Universities of Anhui Province (2022AH010085), the Natural Science Foundation of Anhui Province (2008085MF200), the Natural Science Foundation in Universities of Anhui Province (KJ2021A0970), and the Key Research and Development Plan Project Foundation of Huainan (2021A248).

Data Availability Statement: The data presented in this study are available in the article.

Conflicts of Interest: The authors declare no conflicts of interest.

References

1. Chua, L.O.; Yang, L. Cellular neural networks: Theory. *IEEE Trans. Circuits Syst.* **1988**, *35*, 1257–1290. [[CrossRef](#)]
2. Liu, P. Delay-dependent global exponential robust stability for delayed cellular neural networks with time-varying delay. *ISA Trans.* **2013**, *52*, 711–716. [[CrossRef](#)] [[PubMed](#)]

3. Yang, G. New results on the stability of fuzzy cellular neural networks with time-varying leakage delays. *Neural Comput. A.* **2014**, *25*, 1709–1715. [[CrossRef](#)]
4. Pu, H.; Liu, Y.; Jiang, H.; Hu, C. Exponential synchronization for fuzzy cellular neural networks with time-varying delays and nonlinear impulsive effects. *Cogn. Neurodyn.* **2015**, *9*, 437–446. [[CrossRef](#)] [[PubMed](#)]
5. Duan, S.; Hu, X.; Dong, Z.; Wang, L.; Mazumder, P. Memristor-based cellular nonlinear neural network: Design, analysis and applications. *IEEE Trans. Neural Netw. Learn. Syst.* **2015**, *26*, 1202–1213. [[CrossRef](#)]
6. Yang, T.; Yang, L.; Wu, C.; Chua, L.O. Fuzzy cellular neural networks: Theory. In Proceedings of the IEEE International Workshop on Cellular Neural Networks and Applications, Seville, Spain, 24–26 June 1996; pp. 181–186, 225–230.
7. Li, Z.; Li, K. Stability analysis of impulsive fuzzy cellular neural networks with distributed delays and reaction-diffusion terms. *Chaos Solitons Fractals* **2009**, *42*, 492–499. [[CrossRef](#)]
8. Li, X.; Rakkiyan, R.; Balasubramaniam, P. Existence and global stability analysis of equilibrium of fuzzy cellular neural networks with time delay in the leakage term under impulsive perturbations. *J. Franklin Inst.* **2011**, *348*, 135–155. [[CrossRef](#)]
9. Jia, R. Finite-time stability of a class of fuzzy cellular neural networks with multi-proportional delays. *Fuzzy Sets Syst.* **2017**, *319*, 70–80. [[CrossRef](#)]
10. Duan, L.; Fang, X.; Fu, Y. Global exponential synchronization of delayed fuzzy cellular neural networks with discontinuous activations. *Int. J. Mach. Learn. Cybern.* **2019**, *10*, 579–589. [[CrossRef](#)]
11. Babcock, K.; Westervelt, R. Stability and dynamics of simple electronic neural networks with added inertial. *Physica D* **1986**, *23*, 464–469. [[CrossRef](#)]
12. Mauro, A.; Conti, F.; Dodge, F.; Schor, R. Subthreshold behavior and phenomenological impedance of the squid giant axon. *J. Gen. Physiol.* **1970**, *55*, 497–523. [[CrossRef](#)] [[PubMed](#)]
13. Koch, C. Cable theory in neurons with active, linearized membranes. *Biol. Cybern.* **1984**, *50*, 15–33. [[CrossRef](#)]
14. Angelaki, D.; Correia, M. Models of membrane resonance in pigeon semicircular canal type II hair cells. *Biol. Cybern.* **1991**, *65*, 1–10. [[CrossRef](#)] [[PubMed](#)]
15. Song, C.; Cao, J. Dynamics in fractional-order neural networks. *Neurocomputing* **2014**, *142*, 94–498. [[CrossRef](#)]
16. Kaslik, E.; Sivasundaram, S. Nonlinear dynamics and chaos in fractional-order neural networks. *Neural Netw.* **2012**, *32*, 245–256. [[CrossRef](#)]
17. Chen, L.; Chai, Y.; Wu, R.; Ma, T.; Zhai, H. Dynamic analysis of a class of fractional-order neural networks with delay. *Neurocomputing* **2013**, *111*, 190–194. [[CrossRef](#)]
18. Wang, H.; Yu, Y.; Wen, G. Stability analysis of fractional-order hopfield neural networks with time delays. *Neural Netw.* **2014**, *55*, 98–109. [[CrossRef](#)]
19. Wang, H.; Yu, Y.; Wen, G.; Zhang, S.; Yu, J. Global stability analysis of fractional-order hopfield neural networks with time delay. *Neurocomputing* **2015**, *154*, 15–23. [[CrossRef](#)]
20. Chen, J.; Zeng, Z.; Jiang, P. Global Mittag-Leffler stability and synchronization of memristor-based fractional-order neural networks. *Neural Netw.* **2014**, *51*, 1–8. [[CrossRef](#)]
21. Yan, S.; Gu, Z.; Nguang, S. Memory-event-triggered H_∞ output control of neural networks with mixed delays. *IEEE Trans. Neural Netw. Learn. Syst.* **2022**, *33*, 6905–6915. [[CrossRef](#)] [[PubMed](#)]
22. Lakshmanan, S.; Prakash, M.; Lim, C.; Rakkiyappan, R.; Balasubramaniam, P.; Nahavandi, S. Synchronization of an inertial neural network with time-varying delays and its application to secure communication. *IEEE Trans. Neural Netw. Learn. Syst.* **2018**, *29*, 195–207. [[CrossRef](#)]
23. Yang, X.; Ho, D.W.C. Synchronization of delayed memristive neural networks: Robust analysis approach. *IEEE Trans. Cybern.* **2016**, *46*, 3377–3387. [[CrossRef](#)]
24. Prakash, M.; Balasubramaniam, P.; Lakshmanan, S. Synchronization of Markovian jumping inertial neural networks and its applications in image encryption. *Neural Netw.* **2016**, *83*, 86–93. [[CrossRef](#)]
25. Li, X.; Li, X.; Hu, C. Some new results on stability and synchronization for delayed inertial neural networks based on non-reduced order method. *Neural Netw.* **2017**, *96*, 91–100. [[CrossRef](#)]
26. Gu, Y.; Wang, H.; Yu, Y. Stability and synchronization for Riemann–Liouville fractional-order time-delayed inertial neural networks. *Neurocomputing* **2019**, *340*, 270–280. [[CrossRef](#)]
27. Feng, Y.; Xiong, X.; Tang, R.; Yang, X. Exponential synchronization of inertial neural networks with mixed delays via quantized pinning control. *Neurocomputing* **2018**, *310*, 165–171. [[CrossRef](#)]
28. Tang, Q.; Jian, J. Exponential synchronization of inertial neural networks with mixed time-varying delays via periodically intermittent control. *Neurocomputing* **2019**, *338*, 181–190. [[CrossRef](#)]
29. Liang, K.; Wanli, L. Exponential synchronization in inertial Cohen–Grossberg neural networks with time delays. *J. Frankl. Inst.* **2019**, *356*, 11285–11304. [[CrossRef](#)]
30. Shi, J.; Zeng, Z. Global exponential stabilization and lag synchronization control of inertial neural networks with time delays. *Neural Netw.* **2020**, *126*, 11–20. [[CrossRef](#)]
31. Cui, N.; Jiang, H.; Hu, C.; Abdurahman, A. Finite-time synchronization of inertial neural networks. *J. Assoc. Arab. Univ. Basic Aplied Sci.* **2017**, *24*, 300–309. [[CrossRef](#)]
32. Guo, Z.; Gong, S.; Huang, T. Finite-time synchronization of inertial memristive neural networks with time delay via delay-dependent control. *Neurocomputing* **2018**, *293*, 100–107. [[CrossRef](#)]

33. Wei, R.; Cao, J.; Alsaedi, A. Fixed-time synchronization of inertial memristor-based neural networks with discrete delay. *Cogn. Neurodynamics* **2018**, *12*, 121–134. [[CrossRef](#)]
34. Chen, C.; Li, L.; Peng, H.; Yang, Y. Fixed-time synchronization of inertial memristor-based neural networks with discrete delay. *Neural Netw.* **2019**, *109*, 81–89. [[CrossRef](#)] [[PubMed](#)]
35. Alimi, A.M.; Aouiti, C.; Assali, E.A. Finite-time and fixed-time synchronization of a class of inertial neural networks with multi-proportional delays and its application to secure communication. *Neurocomputing* **2019**, *332*, 29–43. [[CrossRef](#)]
36. Duan, L.; Wei, H.; Huang, L. Finite-time synchronization of delayed fuzzy cellular neural networks with discontinuous activations. *Neurocomputing* **2019**, *361*, 56–70. [[CrossRef](#)]
37. Liu, Y.; Sun, Y. Fixed-time synchronization of fuzzy cellular neural networks with time-varying delays and discontinuous activations. *IEEE Access* **2020**, *8*, 65801–65811. [[CrossRef](#)]
38. Sun, Y.; Liu, Y.; Liu, L. Asymptotic and finite-time synchronization of fractional-order memristor-based inertial neural networks with time-varying delay. *Fractal Fract.* **2022**, *6*, 350. [[CrossRef](#)]
39. Zhao, K. Stability of a nonlinear Langevin system of ML-type fractional derivative affected by time-varying delays and differential feedback control. *Fractal Fract.* **2022**, *6*, 725. [[CrossRef](#)]
40. Zhang, T.; Xiong, L. Periodic motion for impulsive fractional functional differential equations with piecewise Caputo derivative. *Appl. Math. Lett.* **2020**, *101*, 106072.
41. Zheng, M.; Li, L.; Peng, H.; Xiao, J.; Yang, Y.; Zhang, Y.; Zhao, H. Fixed-time synchronization of memristor-based fuzzy cellular neural network with time-varying delay. *J. Frankl. Inst.* **2018**, *355*, 6780–6809. [[CrossRef](#)]
42. Sun, Y.; Liu, Y. Fixed-time synchronization of delayed fractional-order memristor-based fuzzy cellular neural networks. *IEEE Access.* **2020**, *8*, 165951–165962. [[CrossRef](#)]
43. Li, C.; Deng, W. Remarks on fractional derivatives. *Aied Math. Comput.* **2007**, *187*, 777–784. [[CrossRef](#)]
44. Yan, S.; Nguang, S.; Gu, Z. H_∞ weighted integral event-triggered synchronization of neural networks with mixed delays. *IEEE Trans. Ind. Inform.* **2021**, *17*, 2365–2375. [[CrossRef](#)]
45. Yan, S.; Gu, Z.; Park, J.; Xie, X. Synchronization of delayed fuzzy neural networks with probabilistic communication delay and its application to image encryption. *IEEE Trans. Fuzzy Syst.* **2022**, *31*, 930–940. [[CrossRef](#)]

Disclaimer/Publisher’s Note: The statements, opinions and data contained in all publications are solely those of the individual author(s) and contributor(s) and not of MDPI and/or the editor(s). MDPI and/or the editor(s) disclaim responsibility for any injury to people or property resulting from any ideas, methods, instructions or products referred to in the content.